NOVEL PRINCIPLES AND THEIR EFFECTS IN THE DESIGN OF ELECTROSTATIC ACCELERATORS IN ATOMKI

(Compiled by Ede Koltay)

A team of physicists and engineers in ATOMKI ran a research and development project several decades ago with the aim of building up an electrostatic accelerator laboratory, which was to meet the requirements in a broad thematic field on fundamental and applied research with nuclear particle beams in the MeV energy range.

Our former experience in accelerator physics, vacuum technique, and electronics, as well as the critical evaluation of the international literature on electrostatic accelerators helped us in the construction of a 1 MV pilot machine, but to obtain high reliability and flexibility in its application some novel ideas have been applied, as well. Positive experience gathered during test runs and applications in scientific work served as a basis for planning and building up a single ended 5 MV Van de Graaff accelerator. Around both accelerators multi-purpose beam transport systems and dedicated experimental systems have been built up.

These machines as elements of the basic facilities of the Institute play an important role by providing ion beams of energies from a few keV up to 5 MeV for research in various fields of up to date basic and applied sciences. We are continuously improving some features necessary for meeting the needs raised by new types of application.

Below a short summary is given on some of our original results published in accelerator physics as we applied them in designing our machines. Some of these ideas found applications in other laboratories, too.

1. THE OPTIMIZATION OF THE ELECTROSTATIC FIELD OF SINGLE ENDED VAN DE GRAAFF ACCELERATORS

I.1. Kiss, Á., Koltay, E., Szalay, A., NIM 46 (1967) 130-135

The maximum working voltage of an electrostatic generator is reached when the electric field strength on any part of the terminal surface, or on any construction elements nearby, becomes equal to the dielectric strength of the insulating gas in the pressure vessel. Therefore the field strength distribution is to be optimized through the suppression of any local field strength maxima. Single ended generators are housed in a cylindrical pressure vessel terminated by a tori-spherical upper lid. Classically they are equipped with a cylindrical high voltage terminal closed with a matching spherical calotte. The diameter of the cylindrical part equals that of the equipotential rings closing the insulating column. In Figure 1 shown are the minimized electric field strengths on the inner electrodes and in the interelectrode gaps for a spherical and a cylindrical capacitor in a model case (10 cm outer radii and voltage difference of 50 kV). In the spherical and the cylindrical case inner radius 3.68 cm and 5 cm should be used, respectively, to reach the minimal field strength on the inner electrode. The ratio of the respective field strengths amounts to 1.47. It means that a considerable increase appears in the field strength around the connection point of the spherical and cylindrical geometries: i.e. the maximum operating voltage is strongly limited due to the transition from cylinder with zero curvature to hemisphere of non-zero curvature in the meridional plane.

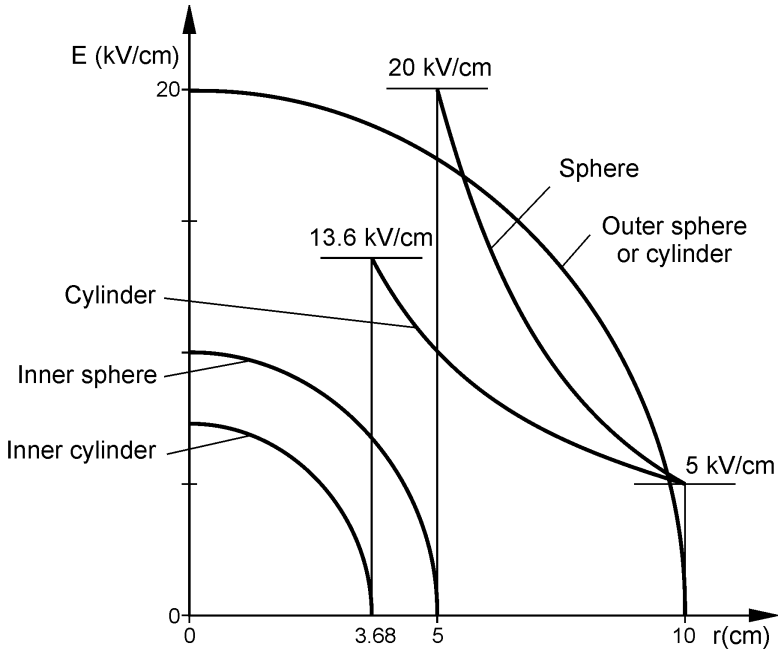

Figure 1

Curve (***a***) in Figure 2 shows the variation of the field strength along the contour of the terminal electrode in the case of our 1 MV generator in classical configuration.

We proposed a substitution of the original configuration with a new terminal. We find inspiration from technical solutions of problems like the ones where straight lines should be smoothly joined to curved lines (e.g. in case of building railway tracks). We attempted as our new terminal shape to choose a third-order paraboloid of rotation closed with a spherical calotte. We hoped to achieve with this arrangement a smooth transition in the meridional plane from the zero curvature to the curvature of the spherical top of the terminal. In the case of ***(b)*** curve the maximum appearing in the field strength at the joint interval is considerably diminished. Further improvement was obtained in the case of curve **(*c*)** representing the actual configuration used in the 1 MV generator, in which the equipotential rings of the insulation column were made of tubes of optimum shaped elliptic cross section in contrast to rings made of circular cross section tubes in the case of configuration ***(b).***

Figure 3 presents the field strength distribution in the case of the 5 MV accelerator, where larger dimensions of the pressure vessel permitted us to end up with field strength minimum with a somewhat diminished outer diameter of the equipotential rings. This means a considerable increase of the maximum generator voltage in the given configuration.

The results of Figures 2 and 3 were obtained with the analog modeling in an electrolytic trough.

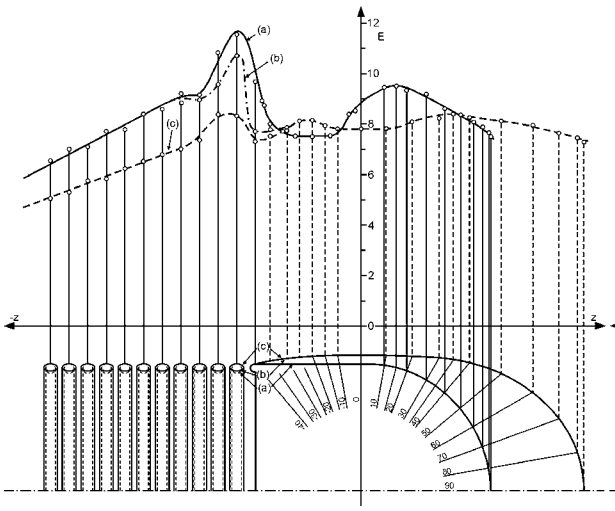

Figure 2

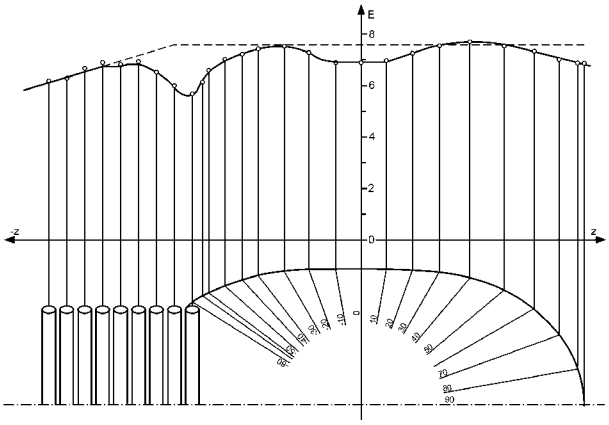

Figure 3

2. VOLTAGE SURGES IN VAN DE GRAAFF GENERATORS

2-1. Kiss, Á.Z., NIM 92 (1971) 361-363

The high voltage construction parts of the accelerator (the terminal in the pressure vessel, as well as the metallic elements of the insulation column, and those of the accelerator tubes) compose a number of high voltage capacitors, which are storing a high amount of electric charge during the run of the accelerator. In the case of an electric breakdown caused by any possible reason at any point of the generator, an avalanche of electric breakdowns is generated between all neighboring elements This process has been modeled for the configuration of the 1 MV machine in calculations using the RC equivalent circuit shown in Figure 4, which contain the voltage divider resistor chain, as well.

As shown in Figure 5 voltage surges jump in electrode gaps along the insulting column. The amplitude of the surges varies with the serial number of the rings given in the horizontal axis. Its amplitude increases with the serial number *f* of the electrode on which a radial spark appears. The amplitude of the transient voltage surge from the uppermost insulating ring in the acceleration tube becomes 17.5 times higher in a breakdown originating on the terminal itself, than the static stress under stable working conditions. The spark-over voltages on the inner and/or outer surfaces of the elements of insulator stacks and on the rings of the acceleration tube are much lower as the dielectric strength of the insulating gas in the vessel. Therefore the surfaces of the glass insulator elements are subjected to strong erosion effects during column transient sparking. The vacuum in the acceleration tube shows sudden degradations in sparking inside the tube. It was the depression of such damaging effect that we were aimed at by lengthening the lower curved portion of the terminals. The result is clearly seen in Figures 2 and 3. The small dimensions of the 1 MV machine prevented us from moderating the field maxima as shown in curves ***(a)*** and ***(b),*** while in the case of the 5 MV machine the uppermost rings, which could have caused the strongest destruction of the insulators, were practically hidden in a broad minimum formed on the field distribution curve. We are convinced that this is the explanation of the fact that we hardly found mechanical destruction in this column section during the total working period amounting to about 60000 hours of operation to date

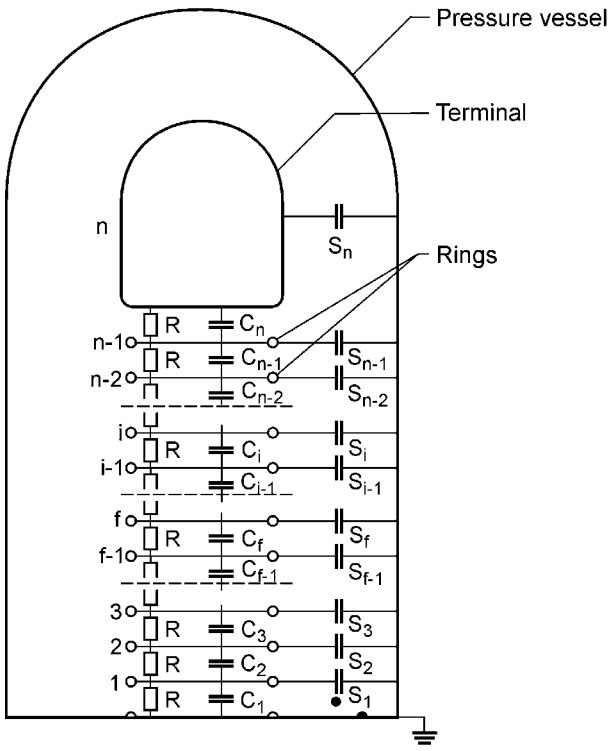

Figure 4

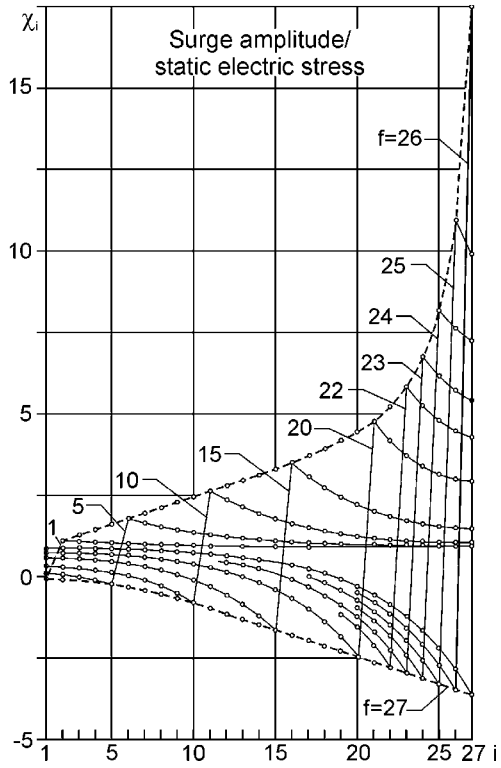

Figure 5

3. ION OPTICS OF ACCELERATION TUBES

3.1. Koltay E., Physics Letters 4 (1963) 66-68
3.2. Gyarmati, B., Koltay E., NIM 66 (1969) 253-260
3.3. Kiss, Á., Koltay, E., Szabó, Gy., IEEE 81CH1639-4 (1981) 103-106
3.4 Kiss Á. Z., Koltay., Papp I.,Szabó., Félszerfalvi J., Nyilas I. NIM 268 (1989) 253-260
3.5. Bartha, L., Kiss Á. Z., Koltay E., Nagy A.,Szabó Gy., Félszerfalvi J. NIM 328 (1993) 253-260
3.6. Bartha, L., Koltay, E., Mórik, Gy., NIM B 111 (1996) 157-160

The construction of the acceleration tube has a determinant influence on the proper working conditions of a Van de Graaff accelerator. The acceleration tube consist of a series of properly shaped metallic electrodes glued between short ring-shaped insulators (e.g. in our case the lengths of interelectrode gaps amount to 30 mm).

Mechanically it withstands the pressure difference between the vacuum in the tube and the pressure of the insulating gas in the vessel. Electrically it is stressed by the total voltage along the tube length.

From electron-optical point of view the tube structure plays twofold roles. On the one hand it focuses the injected ions in a paraxial beam of prescribed diameter. On the other hand it limits the flight length of the secondary electrons released from the tube electrodes and/or from the rest gas molecules in the tube vacuum and get accelerated towards the upper tube end. The impact of the electrons in the tube generates disturbing high intensity energetic bremsstrahlung. The current of the tube electrons together with that of charged particles released by the absorption of X-rays in the pressurized insulation gas represent additional load in the current balance of the generator.

The limiting of the bremsstrahlung effects can be achieved by dividing the tube into sections of properly selected lengths with alternating opposite direction of transversal

extraction field components which are superimposed on the longitudinal accelerating field. Such sections produce a strong deflection of the electrons due to their low mass and practically zero initial energy, while the perturbation caused on the heavier and more energetic ions can be kept in narrow limits. An alternative tool can be obtained through the modulation of the axial field gradient by inserting some short gaps of zero field strength between the accelerating electrodes. This acts as divergent electron optical lenses on the electrons. In such a way the majority of the electrons can be trapped without any deflection effect exerted on the ions.

Different electrode configurations can be used for an optimum solution of the above problem. In Figures **6 (a), (b),** and **(c)** shown are accelerator tube versions with inclined field, spiraling field, and axial field modulation, respectively, used alternatively in our 5 MV accelerator, according to the special needs of different on-going experiments.

Part of the ions scattered in the tube can build up surface charges on the insulating wall of the tubes, which may cause unforeseeable fluctuations of the beam position at the tube exit. To avoid this effect use was made of dish-shaped electrodes in some cases, which exert screening of the insulator surfaces.

The electron optical behavior of the above tube versions have been investigated and optimized on the basis of calculations of the ion and electron trajectories in various cases. The results of the model calculations have been checked through the realization of the different versions and conclusions were drawn for the optimum configuration to be selected for a given type of experiments. For an easy rearrangement of the optical configuration of the tube, intermediate grooved electrode holding rings were used and the actual electrode plates were fixed into the grooves by a slight elastic deformation of the plates.

(a) (b)

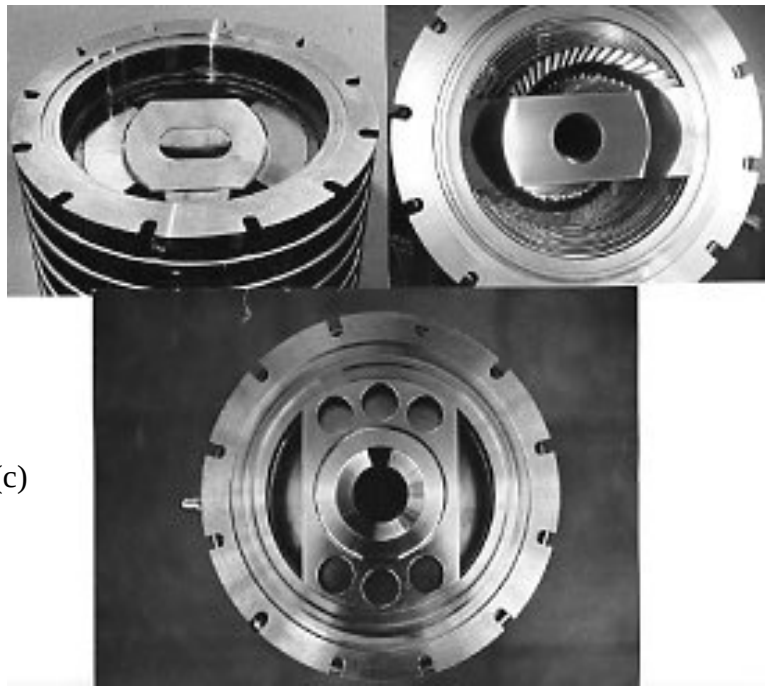

(c)

Figure 6

With the removal of all the electrode plates from a tube section an ample internal channel was obtained, with made it possible to remove the impurity layer which have been built up during an operation of more than 20000 hours on the insulation wall of the tube. An abrasive blast cleaning technology using silicon carbide dust of 0.4mm granulation was found to be appropriate to increase the operational time of worn-out tube sections.

4. OPTICAL BEHAVIOR OF ACCELERATION TUBES STUDIED IN BREMSSTRAHLUNG MEASUREMENTS

4.1. Kiss, Á.Z., Koltay E., Szabó Gy., NIM 117 (1974) 325-329
4.2. Kiss, Á.Z., Koltay E., Papp, I., Szabó Gy., Félszerfavi. J., Nyilas I. NIM A268 (1988) 382-385,
4.3.Friedrich, M., Günzel, R,, Kiss, Á. Z, Koltay E., Félszerfalvi J. NIM A234 *(1985)*1-5

Measurements have been performed for the mapping of the longitudinal distribution of the bremsstrahlung background generated by secondary electrons in the tube configurations with different electron extraction properties mentioned above. A strongly shielded scintillation detector placed behind a narrow collimator was mounted on a platform of a fork lift movable parallel with the tube axis. Additionally thermoluminescent dose meter capsules (TLD-s) were fixed on the outer wall of the pressure vessel along the generating line nearest to the tube axis.

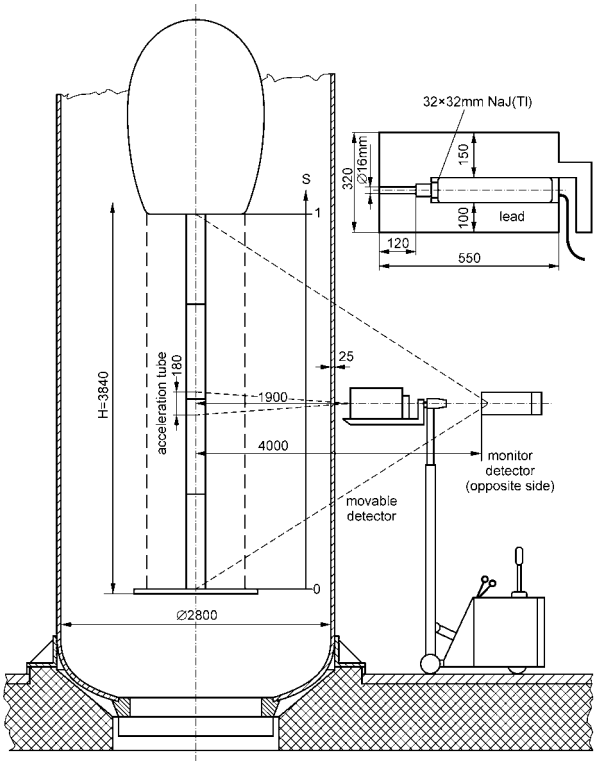

Figure 7

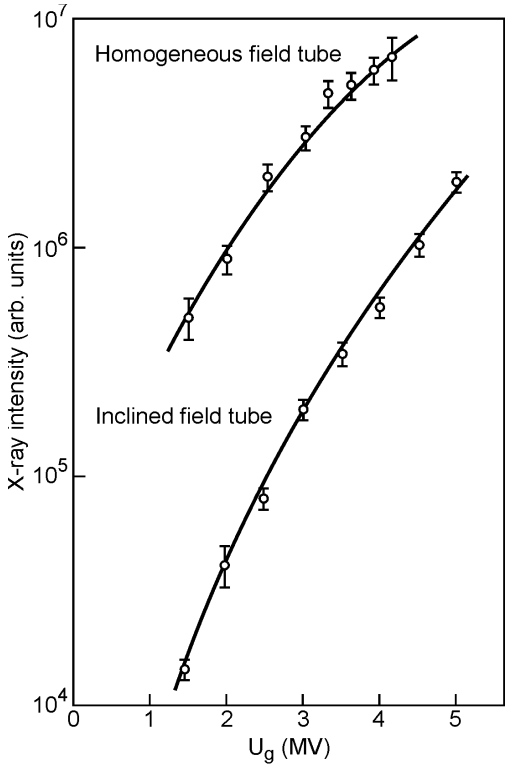

Figure 8

The data obtained with the scintillation detector directly measured the bremsstrahlung intensity, while an estimate has been drawn on the end point energy of the X-ray distribution through the evaluation of the spectra at a given longitudinal position in the tube. Evaluation of TLD-s was used for the determination of absolute dose intensities. To eliminate the absorption of the vessel wall *in situ* dose intensities have been mapped, too. To this aim a set of TLD-s has been put into a high number of tube construction elements at a distance of 20 cm from the tube axis.

The experimental set-up for scintillation measurements is shown in Figure 7. In Figure 8 some results taken for classical tube configuration without electron extraction traps and for. an inclined field acceleration tube configuration are shown in arbitrary units.. In Fig.9 absolute dose intensity curves are shown for screened homogeneous and spiraling sector tubes measured by TLD dose meters on the outer vessel walls. The two upper curves in Figure 10 show *in situ* dose intensity distribution curves along a tube of axial field modulation

containing eight short circuited trapping sections. The reproducibility of the measurements is checked in two subsequent runs with one *(single TLD)* and two *(twins)* TLD-s, respectively, placed at the same positions near the outer wall of the acceleration tube. The maxima on the curves clearly represent the efficient stopping of the secondary electrons near the traps. They are only weakly observable in the curves taken on the outer vessel wall due to the fact that the majority of the electrons get accelerated by only one eighth of the total accelerating voltage, and the vessel wall reduces intensively the low energy bremsstrahlung generated during the stopping of the electrons.

Our beam diagnostic method has been applied in the frame of an international collaboration for testing beam optics in the tubes of the tandem accelerator of the Nuclear Physics Institute in Dresden, Germany, too.

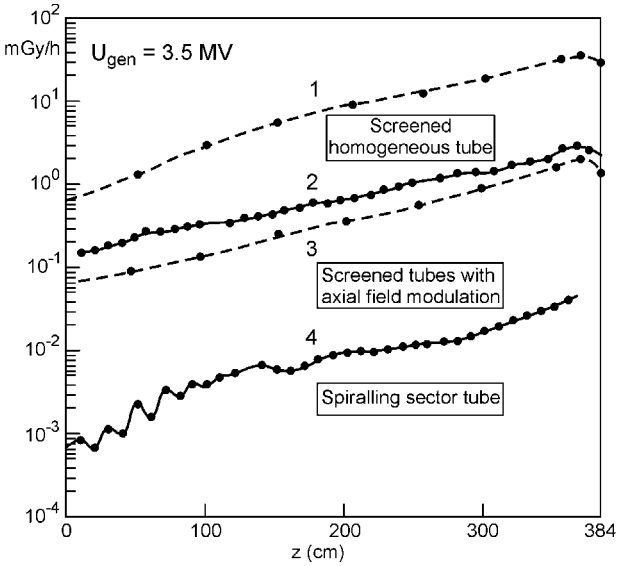

Figure 9

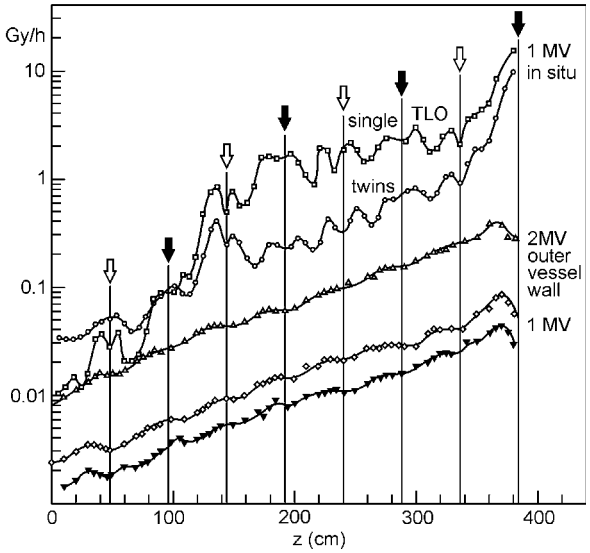

Figure 10

5. ASYMMETRIZED QUADRUPOL LENSES IN THE BEAM TRANSPORT SYSTEMS OF VAN DE GRAAFF ACCELERATORS IN ATOMKI

5.1 Koltay E., Szabó Gy., NIM 35 (1965) 88-92
5.2 Ovsyannikova, L., P., Yavor, S., Ya., Koltay E., Szabó Gy., NIM 74 (1969) 185-190

The accurate definition of the position and direction of the ion beam at the exit of the accelerator and in the entrance points to optical elements and experimental facilities plays a determinant role. This guarantees the high accuracy and sensitivity in the experimental application of the accelerated beam. Also, it is the solution to this that makes possible the steering of the beam through the narrow slits of the analyzing magnet used in measuring and stabilizing the beam energy with a typical relative accuracy of 10^{-4}. Furthermore, the requirements concerning the beam size, beam position, and paraxiality in ion microprobe applications are even more stringent. The necessary precision is determined by the object slit of the width of 10μ order of magnitude and of the strict optical conditions to minimize the aberration of the image size on the target.

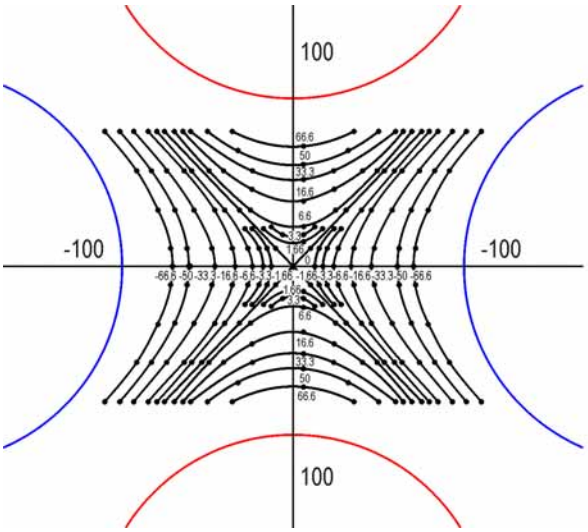

Figure 11

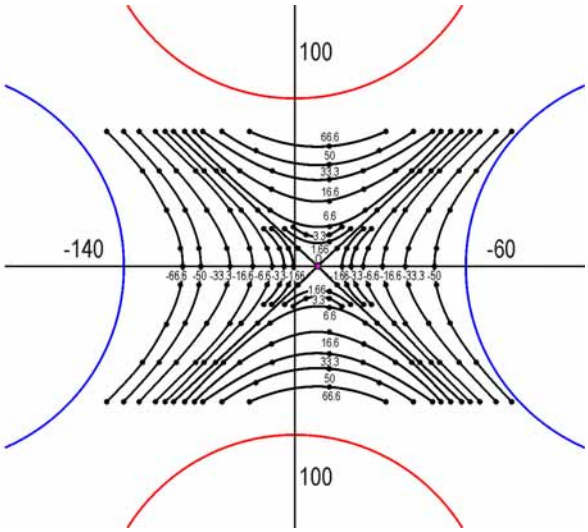

Figure 12

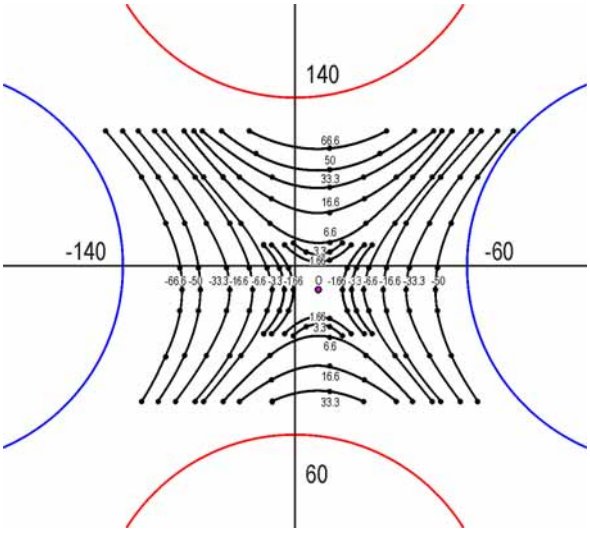

Figure 13

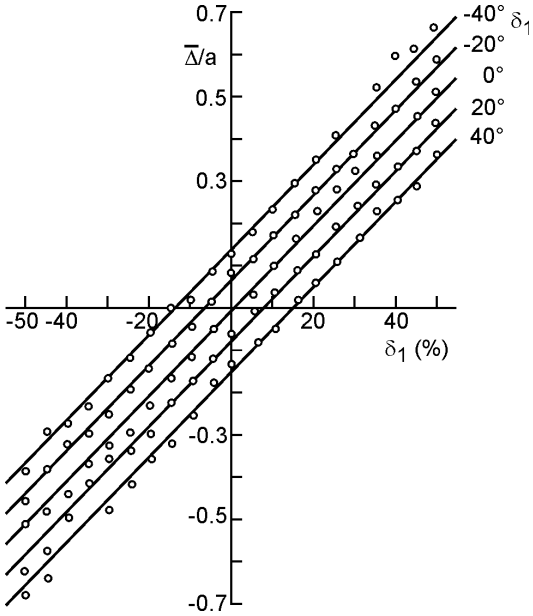

Figure 14

To adjust independently the beam position and the beam direction along two transversal axes perpendicular to each other, as a rule people use in both directions two electrostatic or magnetic beam deflection elements. Furthermore, they normally achieve a stigmatic focusing of the beam into an image plane by the aid of two strong focusing astigmatic elements (i.e. a quadrupole lens doublet). The four-parameter steering and the two-parameter focusing are conventionally solved by applying independent steering and focusing system with six adjustable parameters altogether. In a multi-purpose accelerator laboratory the beam steering and beam focusing systems are to be set up both before and behind the analyzing magnet, and in each channel of the beam transport system behind the switching magnet.

In the case of our Van de Graaff accelerators we united the steering and focusing functions by the use of asymmetrized quadrupole doublets. That means, we superimposed two dipole fields on each lens of a quadrupole doublet by deliberately upsetting the conventional

symmetry in the feeding of the four poles in the lens, through slightly increasing and decreasing the pole strengths in the opposite poles. The focal length of the lens remain practically unchanged, while the two adjustable asymmetry parameters perform the necessary beam shifts in two perpendicular directions. As shown in Figures 11, 12, and 13 the asymmetrization is practically equivalent to transversal mechanical shifts of the lens in one or two directions. By applying this arrangement on both lenses of a doublet the task of adjusting the above mentioned six parameters can be solved by two optical elements only. The dependence of the beam shifts on the asymmetry parameters δ_1 and δ_2 is linear. This is demonstrated in one of the deflection planes in Figure 14.

Before the entrance slits of the analyzing magnet an asymmetrized electrostatic quadrupole doublet is used, while asymmetrized magnetic quadrupole doublets serve at the entrance to the switching magnet and on each beam transport tube.

Detailed theoretical investigations have been performed to clear up how much the optical aberrations of a quadrupole doublet is increased by field distortions introduced with the superimposition of dipole components. These calculations as well as experimental observations show, that the consequences of this novel arrangement are not significant.

6. LIGHT ATOMIC AND MOLECULAR BEAMS ACCELERATED IN VAN DE GRAAFF ACCELERATORS OF ATOMKI

6-1. Nagy J., ATOMKI KÖZLEMÉNYEK 7 (1965) 209-
6-2. Kiss I., Koltay E., Bornemisza-Pauspertl P., Revue de Physique Appliqueé 12 (1977)1481-1495
6-3. Bartha L., ,Kiss, Á.Z., Koltay E., Szabó Gy., NIM A287 (1990) 156-160
6-4. Bartha L., Kiss, Á.Z., Koltay E., Szabó Gy., Zolnai, L., Nyilas, I. NIM A244 (1986)166–169
6-5 Hunyadi I.,. Kiss, Á.Z., Kiss, I., Koltay E., Szabó Gy., NIM 220 (1984) 154-157

Instead of the ion extraction system of Thonemann type conventionally used in the radiofrequency ion sources in Van de Graaff accelerators, we implemented a cathode lens extraction system proposed by Baily and Ward. With this modification the electric erosion on the bottle wall and the leaks often appearing at the metal-to-quartz seals were fully eliminated. On the other hand, high mechanical accuracy achieved in machining the extraction electrode, easy modification of its dimensions as well as easy replacement of the used cathode tips resulted in high quality stable beam together with the necessary flexibility for running the source with different gases. The structure of the source is to be seen in figure 15.

Experiments in ion-atom collision physics often need light atomic and molecular beams in various charge states, or that of neutral particles. High cross sections in atomic processes permit the use of low intensity beams sometimes even in nanoAmpere range. Our finding was that different atomic and molecular beams can be produced with typical intensities given (in nA units) in the table by increasing the frequency of the exciting oscillator from the conventional value of 47.5 MHz to 78 MHz and by using appropriate working gases. Charged beams subjected to stripping processes in a foil or gas target then cleaned from the remaining charged particles in deflecting magnetic field can result in neutral beams. The same technique can be applied for getting ions of charged states different from that used during the acceleration.

PARTICLE	WORKING GAS IN THE ION SOURCE					
	He	N	Ne	CH_4	CO_2	Freon 12
$3H^+$	-	-	-	900	2,4	-
$3H^{2+}$				1		
$2H^+$		28		4000	2	
H+	220	130	-	500	50	-
He^+	2800	-	-	-	-	-
$2H^+$ és He^{2+}	20	-	-	-	-	-
$2C^+$						40
C^+	-	-	100	10	150	40
C^{2+}	-	-	-	1,5	8	12
$(C3H\ C2H)^+$				270		
$C4H^+$				1300		
$C3H^+$				800		
$C2H^+$				400		
CH^+				10		
$C3H^{2+}$				1,7		
$C2H^{2+}$				3		
CH^{2+}				1,4		
C2O					1000	
$3N^+$	-	2,7	-	-	-	-
$2N^+$	-	1030	-	-	-	-
N^+	-	1300	80	-	25	-
N^{2+}	-	70	-	-	-	-
O^+	-	140	200		80	
O^{2+}	-	-		-	7	-
F^+	-	-	-	-	-	200
F^{2+}	-	-	-	-	-	50
$2Ne^+$	-	-	100	-	-	-
Ne^+	-	-	1000	-	-	-
Ne^{2+}	-	-	20	-	-	-
Cl^{2+}	-	-	-	-	-	22

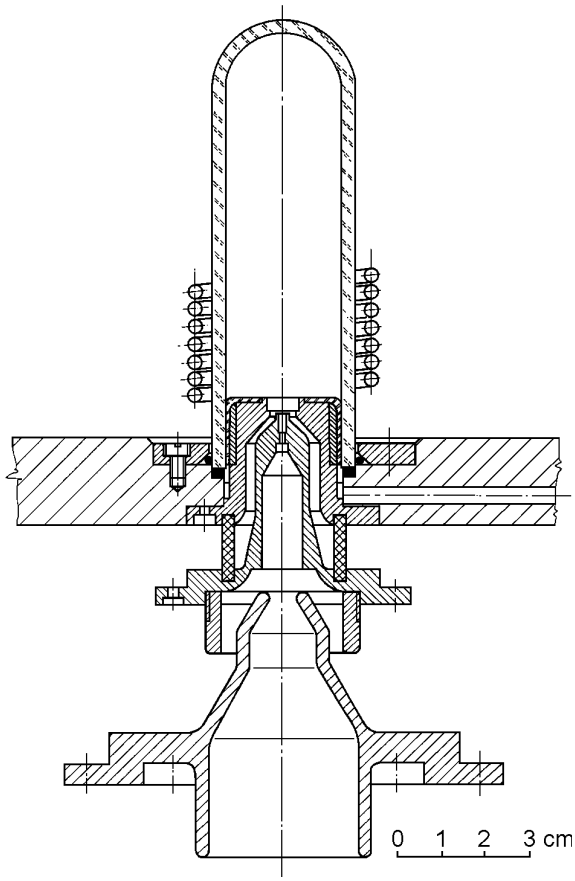

Figure 15

NOTE: A Technical Report of the Van de Graaff accelerators are given in the following articles published in the issues of the journal ATOMKI Közlemények.

VDG-5: **16** (1974) 181-192, **17** (1975) 121-145, **18** (1976) 1-23, **19** (1977) 379 396, **20** (1978) 89-111, **20** (1978) 181-2, **20** (1978) 263-277

VDG-1: **11** (1969) 125